An experimental assessment of torsional and package vibration in an industrial engine-compressor system

B Halkon[1], I Cheong[2], G Visser[2], P Walker[1] and S Oberst[1]
[1]Centre for Audio, Acoustics and Vibration, Univ. of Technology Sydney, Australia
[2]ALS Industrial, Queensland, Australia

ABSTRACT

An experimental field vibration measurement campaign was conducted on an engine-compressor system. Torsional vibrations were measured using both a strain-gauge based technique at the engine-compressor coupling and a rotational laser vibrometer at the torsional vibration damper. Package vibration measurements were simultaneously captured using a number of accelerometers mounted at various locations on the engine and compressor casings. Findings from the study include the observation that the coupling/damper dominant order 1.5 torsional vibration level was higher at idle (c14.1 Hz) than at full speed (c19.1 Hz) and that this is likely the result of the coincidence of the first torsional natural frequency (c19-20 Hz); vibration remained within limits. The package vibration observed was in general within limits and displayed the expected behaviour when shaft speeds coincided with structural resonances. Increasing of system load was observed to result in package vibration level increase in the engine but reduction in the compressor and this is suspected to be as a result of the effect of increased damping. Induced cylinder misfire scenarios were shown to lead to higher vibration levels. To the authors' knowledge, this is the first time that angular displacement, vibratory torque and package vibration have been simultaneously measured, analysed and reported in an industrial context/scenario. It is hoped that this contribution might, therefore, serve as a practical guide to vibration engineers that wish to embark on similar campaigns.

1. INTRODUCTION

Experimental vibration analysis has long been accepted as the most effective means of determining the health of rotating machinery (1), (2). Vibrations in rotating machinery are inevitable but their consequences extend from loss of efficiency through to safety-critical failures. Organisations relying on production processes powered by rotating machinery systems invest heavily in systems and services to monitor vibrational performance. Vibration velocity is generally regarded as the optimum measurement parameter, whether translational or rotational, but often assessment criteria might be specified as displacement or acceleration as well or instead with this choice often influenced by historical factors such as transducer availability, reliability and value proposition or data acquisition or processing options.

Direct shaft measurements are generally more challenging than those from nearby non-rotating components, often requiring significant production downtime and risk management for setup and installation. Slip rings or telemetry required to power transducers and/or transfer signals to non-rotating acquisition systems require larger installation package space and regular maintenance (3). Inevitable aspects such as shaft run-out or eccentricity and whole-body vibration present challenges with proximity probe type solutions and with tachos or encoders which, in addition to the measurement of torsional vibration, are generally used to post-process fixed sampled frequency data as engine order spectra or, indeed, for resampling into the angle domain. Even more the contemporary laser vibrometry (4), insensitive to shaft shape variation and translational vibration, is not the ideal rotating machinery transducer due to speckle noise and vibration component cross-sensitivity challenges (5).

This study has, for the first time, employed a range of rotating machinery applicable transducers and processing techniques simultaneously to better understand the links between torsional and package vibration characteristics for different operating conditions in an industrial context. Comparisons are made between torsional vibration measurements made directly from the torsional damper, using a laser vibrometer, and from the coupling and gearbox input shaft, using a torsional strain gauge configuration. Package vibrations, simultaneously captured at a series of locations on both the engine and compressor using a combination of uni- and tri-axial accelerometers mounted, are examined. Results are assessed, in the context of relevant industry standards/OEM guidelines, to understand the contributing factors towards possible excessive torsional vibration failure and to identify package vibration measurement locations that exhibit correlation to high torsional vibrations.

2. METHODOLOGY

2.1 Machinery arrangement and instrumentation configuration

The system consists of a 12-cylinder gas engine and an oil-flooded screw compressor, the two sub-systems being coupled by a shrink disc flexible rubber coupling with a "2:1" gearbox (116:59 teeth) at the compressor input (Figure 1). The compressor male and female rotors consist of 6 and 4 lobes respectively, thereby meshing at a 1.5:1 ratio. Anticipated dominant vibration frequencies of the system are therefore at engine half orders, 1.97x (1x male rotor), 1.31x (1x female rotor), 7.86x (1x lobe pass frequency, LPF) and 15.73x (2x LPF). The engine is mounted onto a foundation via adjustable chocks at six locations with the compressor being similarly mounted at four locations. Compressor loading is adjusted by varying the position of a slide valve from fully open (0% - unloaded) through fully closed (c100% - full load).

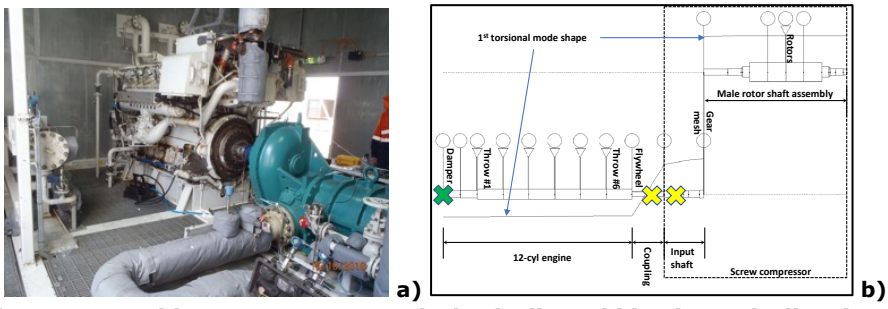

Figure 1 – Machinery arrangement a) physically and b) schematically, also showing 1st torsional mode shape, laser vibrometer (green cross) and strain gauge (yellow cross) measurement locations

A previously commissioned torsional system dynamic analysis, utilising the model shown in Figure 1b, determined the first torsional mode shape as identified. The twist node occurs in the flexible rubber coupling while the antinode appears at the front of the engine near the harmonic damper. The torsional vibration measurement locations (Figure 1b and Figure 2) were therefore chosen to be as sensitive as possible to the drivetrain predicted response, i.e. strain gauges installed at the region of highest stress, i.e. at the coupling nodes (Figure 2a), and laser vibrometer measurement taken at the region of greatest twist angle, i.e. at the damper anti-node (Figure 2b).

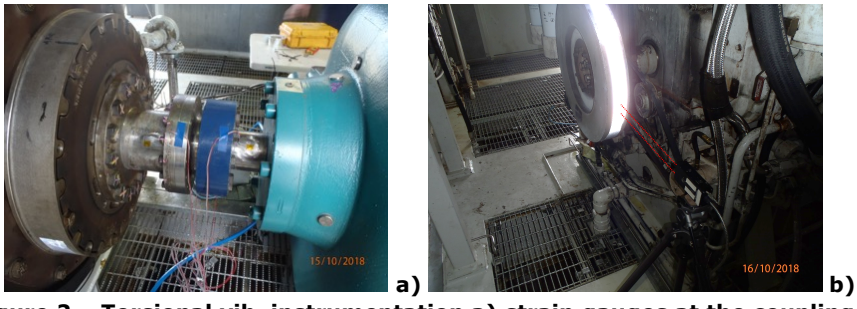

Figure 2 – Torsional vib. instrumentation a) strain gauges at the coupling spacer and gearbox input shafts and b) laser vibrometer, beams highlighted

2.2 Instrumentation configuration
Torsional strain at the coupling was monitored using foil type strain gauges (HBM 350 Ω, Darmstadt Germany; (6)), which were wired in a torsional full bridge, temperature-compensated configuration. The signals from the torsional strain gauges were conditioned using a torque telemetry system (Binsfeld TT10k, MI; (7)) configured with a 500 Hz low-pass filter and transmitter/receiver gains of 2000. Bridges were zeroed and shunt calibrated prior to data acquisition commencement.

Torsional vibration at the damper was directly monitored using a rotational laser vibrometer (Polytec RLV-5500, Waldbronn, Germany; (8)). The damper surface was treated with a 25 mm strip of retro-reflective tape (Figure 2b) to ensure reliable optical signal level. Angular velocity (100 °/s/V), displacement (1 °/V) and RPM (1000 min^{-1}/V) outputs were captured with the RPM and tracking filters set to "Slow".

Package vibrations were recorded using 50 mV/g tri-axial accelerometers (Kistler, NY (9)) and 100 mV/g uni-axial accelerometers (CTC, NY (10)) at locations and in orientations as set out in Table 1. All sensors were magnet mounted to the surface of the selected locations with a frequency response of up to at least 1 kHz expected (11). The following axis convention was used: *x* – axial, parallel to shaft rotation axis; *y* – horizontal, perpendicular to shaft axis, *z* – vertical.

Table 1 – Accelerometer identification and mounting locations

ID	Label	Description	Type	Orientation
A1	E1H+V+A	Engine NDE Block, Above Mount - Male	Triaxial	X, Y, Z
A2	E2H+V	Engine DE Block, Above Mount - Male	Triaxial	Y, Z
A3	E3H+V+A	Engine DE – Shaft Centreline	Triaxial	X, Y, Z
A4	E4H	Engine mid-span block – Male	Uni-axial	Y
A5	E5H	Engine mid-span block – female	Uni-axial	Y
A6	E6H	Engine NDE Block, Above Mount - Female	Uni-axial	Y
A7	E7H	Engine DE Block, Above Mount - Female	Uni-axial	Y
A8	C1H+V+A	Compressor DE – Shaft Centreline	Triaxial	X, Y, Z
A9	C2H+V+A	Compressor Mid-span Casing Top	Triaxial	X, Y, Z
A10	C3H+V+A	Compressor Suction	Triaxial	X, Y, Z
A11	C4H	Compressor Mid-span Casing Female	Uni-axial	Y
A12	C5H	Compressor Mid-span Casing Male	Uni-axial	Y
A13	C6A	Compressor Male Rotor – Axial	Uni-axial	X

Dynamic torque, torsional vibration, package vibration and tachometer data (from the gearbox input shaft) were simultaneously collected via a multi-channel acquisition system (National Instruments cDAQ-9178/NI-9234/NI-9232; (12)). Data were collected in "raw", voltage format with a sampling frequency of 2.048 kHz, yielding a maximum observable frequency of 800 Hz, and recorded to disc in .tdms file format. Data post-processing was subsequently implemented in MATLAB.

2.3 Data post-processing
Torsional strain data were converted to torque, T, through the following equation:

$$\mathbf{T = \mu \varepsilon J G R} \quad (1a)$$

where μ = 2, ε = torsional strain, $\boldsymbol{J}$ = polar moment of inertia, $\boldsymbol{R}$ = radius and $\boldsymbol{G}$ = shear modulus (typically taken as 79 GPa for steel). A two second moving median filter was used to extract the static torque component from the resulting dynamic torque signal with this converted to steady state engine power, P (in kW), as follows:

$$\mathbf{P = T \times RPM / 9548.8} \quad (1b)$$

The dynamic torque component was extracted using a 2 Hz, 10^{th} order Butterworth high-pass filter. Where data were captured during steady-state conditions, frequency response characteristics were investigated by applying a Fast Fourier Transform (FFT) algorithm to four second segments of data, yielding 0.25 Hz spectral resolution, with a Hann window utilised to minimise spectral leakage. Where possible and ideally during sufficiently slow-speed run-ups, order maps, with a minimum resolution of 0.25, were generated showing vibratory torque as a function of both engine speed and frequency.

Since the precise integration filter characteristics were uncertain, instead of using the

available LDV output, angular *displacement* data were determined in post-processing from the LDV angular *velocity* output. A cumulative trapezoidal numerical integration technique, coupled with a 10th order Butterworth (2 Hz) high-pass filter to remove any integration drift ("edge effects" were ignored), was implemented. Again, for (pseudo) steady-state data, frequency spectra and order maps were similarly generated.

Accelerometer signals were 10th order Butterworth (1-800 Hz) bandpass filtered with the resulting signal integrated for velocity, again using a cumulative trapezoidal technique plus 2 Hz high-pass filter and edge-effects removal. Overall package vibration was assessed by computing the running RMS over a 5 sec period with the trend(s) plotted to assess severity against the relevant standard limits (13), (14). Waterfall plots with two averages per spectrum with 0.5 Hz resolution were generated to assess the dynamic package vibration at various timeframes during operation. Operational Deflection Shapes (ODS) were generated from both time and frequency domain data using ModalView (ABSignal; (15)). The former enables investigation of the package vibration response to transient events, e.g. load changes; the latter allows investigation of specific dominant vibration frequencies under steady-state conditions.

2.4 Vibration assessment criteria

Torsional vibration assessment criteria, presented in Table 2, were derived from the aforementioned torsional system dynamic analysis (vibratory torque amplitude of the various shafts in the drivetrain) and from the engine manufacturer service documentation (angular displacement amplitude at the harmonic damper housing).

Table 2 – Torsional vibration acceptability limits, a) vibratory torque and b) angular displacement

a)

System	Location / Condition	Nm (pk-pk)
Engine	Front drive	13219
	Crankshaft	38626
Compressor	Input shaft	6193
	Male rotor shaft	2106
Coupling	Nominal	7002
	Warm	4201

b)

Order (of engine speed)	Deg (pk-pk)
0.5	2.5
1.0	0.7
1.5+	0.3

Package vibration assessment criteria, set out in Table 3, were determined from a combination of the engine manufacturer, ISO 10816-6 (13) and API 619 (14).

Table 3 – Package vibration acceptability limits, velocity-based

Source/standard	Component	mm/s (RMS)	
		Low Alarm	High Alarm
Engine manufacturer	Engine	18.0 (Rough)	26.9 (Very rough)
ISO 10816-6 Class III	Engine	11.2 (Zone B/C)	17.8 (Zone C/D)
API 619	Compressor	8.0 (Concern)	12.0 (Alarm)

3. RESULTS

3.1 Engine performance

The engine performance data shown in Figure 3 are typical for the system under test under normal running conditions. Figure 3a shows the performance for 0% slide valve position, i.e. unloaded, initially with the engine running at low idle (~845 rpm) and subsequently at high idle (~1185 rpm). Figure 3b shows the same initially but, following a brief period at high idle, the slide valve position is progressively increased in 20% increments to full load. The engine achieved a power output of approximately 560 kW during high idle (full speed, no load) conditions. An approximately proportional relationship between valve position and power output can be seen in Figure 3b where, at the maximum slide valve position (full load), the engine achieves a power output of approximately 1070 kW, closely matching its nominal power rating.

3.2 Torsional vibration performance

3.2.1 Vibratory torque

Vibratory torque data at the coupling spacer and gearbox input shafts were interrogated at the following running conditions: low idle, high idle and at full speed under full load. Figure 4a&b show example time waveforms and corresponding FFTs for the measured data at the coupling shaft only at low idle (a) and under full load

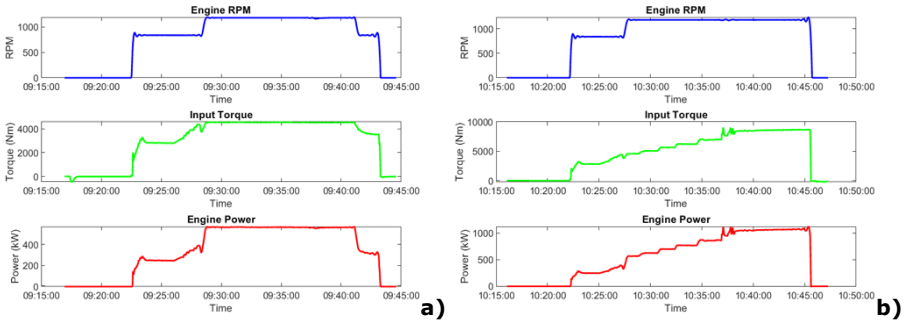

Figure 3 – Typical engine performance a) low and high idle and b) low and high idle, up to full load

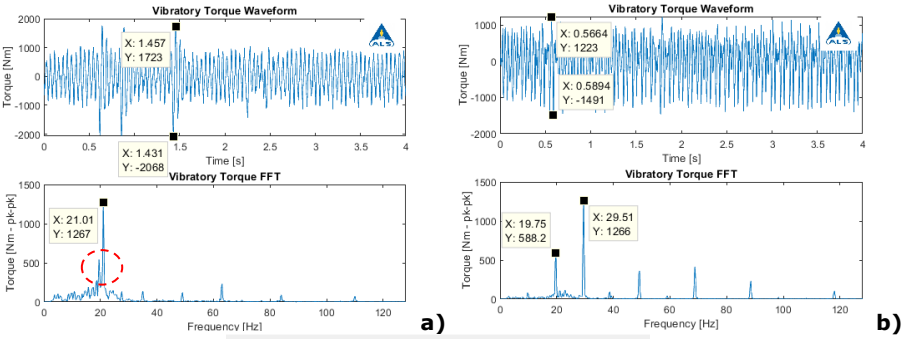

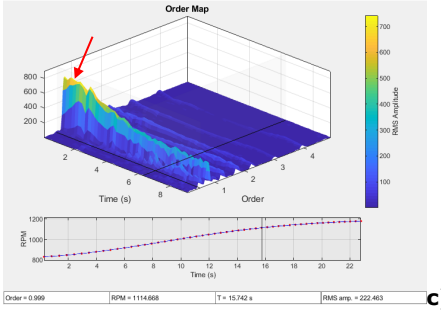

Figure 4 – Vibratory torque at the coupling spacer a) at low idle, b) for full load and c) order map (0.25 res.) for no-load run-up; note order 2.5 peak

conditions (b). The high idle, unloaded signals were of similar form to those observed at full load albeit with reduced levels and are therefore not shown here for the sake of brevity. Similarly, the corresponding signals for the gearbox input shaft, which only show different levels again, are not shown. The FFT representation indicates a dominant frequency at order 1.5 with associated half order harmonics. At low idle, the order 1.5 peak was particularly pronounced whereas at high idle through to full load this dominance was reduced with the order 1 peak becoming increasingly significant as shown in the order map of Figure 4c and as highlighted by the arrow.

The presence of an additional peak at about 19-20 Hz in the low idle FFT (see highlighted region in Figure 4a), suggests that there may be a torsional resonance within this range. The presence of the first torsional natural frequency coinciding within 19-20 Hz would explain the higher vibratory torque response at low idle versus at high idle. This is shown in Table 4 which captures the vibratory torque response for both the coupling spacer and gearbox input shafts at the three running conditions (gearbox input under full load N/A due to loss of data). Despite this, with respect to Table 2a, the system was operating within vibratory torque limits in all cases.

3.2.2 Angular displacement

Specific regions in the data were interrogated to extract the torsional vibration in the form of angular displacement ("position") at the damper housing, under the following conditions: low idle and high idle; various slide valve positions up to (almost) full

Table 4 – Vibratory torque response at coupling spacer and gearbox input

Speed (RPM)	Condition	Torque (Nm pk-pk)	
		Coupling spacer	Gearbox input
845	Low idle	3791	4485
1185	High idle	1734	1861
1185	Full load	2714	/

load; and inducing up to two cold cylinders in the engine followed by varying the slide valve positions. Example torsional vibration FFT data at the harmonic damper are presented in Figure 5. Upon reviewing all data, it was determined that, during normal operating conditions, the angular displacement responses at orders 0.5 and 1.0 were below the limits. The response at order 1.5 was again dominant and approached the acceptability limit of 0.3 deg pk-pk under some conditions, as shown in Figure 6.

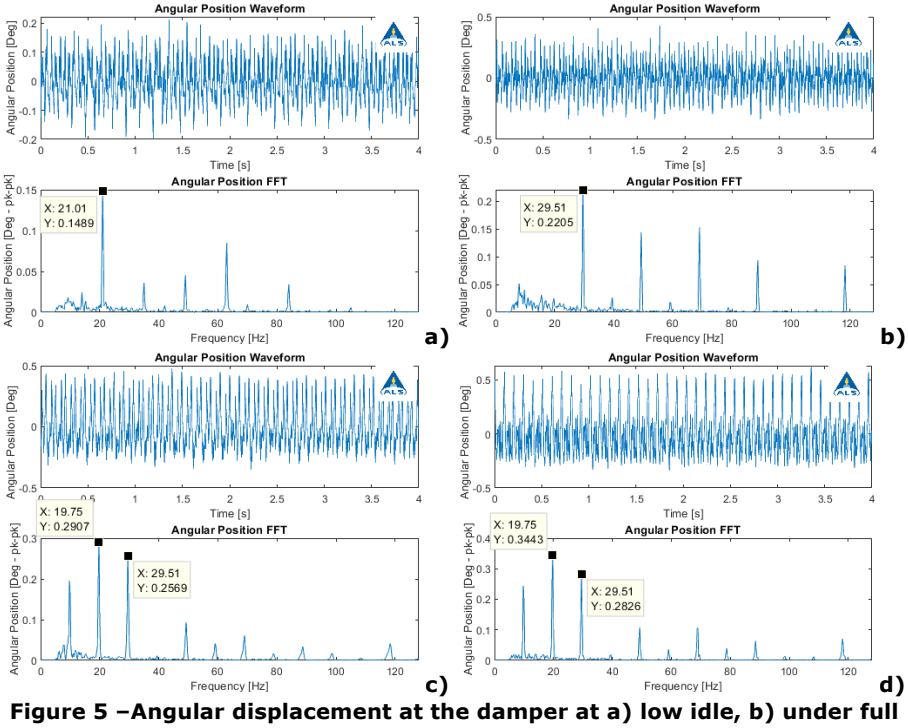

Figure 5 –Angular displacement at the damper at a) low idle, b) under full load, c) with two cold cyls. at high idle and d) with one cold cyl. at full load

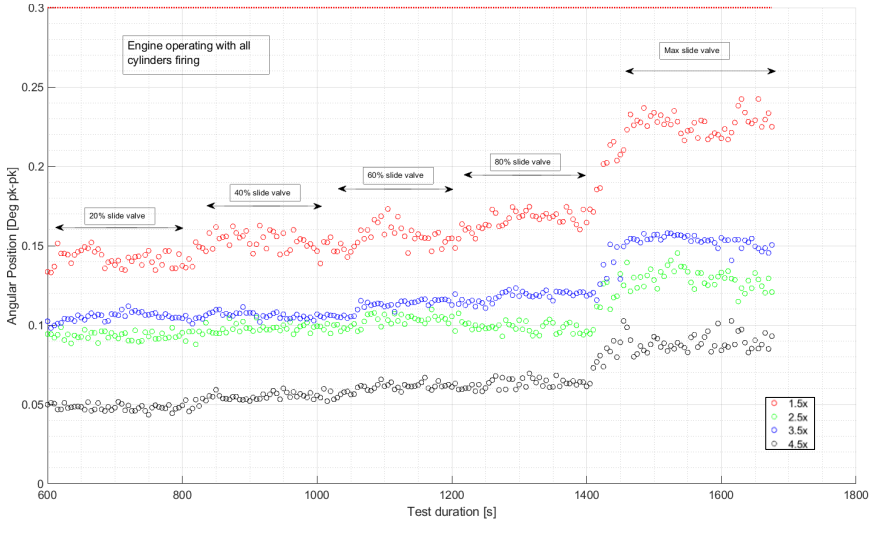

Figure 6 – Order peak values under normal operating conditions

The effect of cold cylinders can also be seen in Figure 5c&d with Table 5 summarising the angular displacement response under all running conditions. A significant increase in order 1.5 vibratory angular displacement of approximately 75% can be observed as one cold cylinder was induced. When a second cold cylinder was induced, an increase of approximately 220% results. In addition to the order 1.5 changes, the increased significance of the order 0.5 and 1 peaks is evident as shown in Figure 5c&d, with the order 1 peak becoming dominant in both cases. While running with two cold cylinders under loaded conditions was not performed following a risk assessment, based on these findings it is likely that the vibratory angular displacement with two cold cylinders under load would result in levels beyond the acceptability limits at 1.5, if not also at other orders.

Table 5 – Angular displacement response at damper housing at order 1.5

Speed (RPM)	Condition	Deg (pk-pk)
845	Normal, unloaded (low idle)	0.19
1185	Normal, unloaded (high idle)	0.12
1185	Normal, 20% slide valve	0.14
1185	Normal, 40% slide valve	0.15
1185	Normal, 60% slide valve	0.16
1185	Normal, 80% slide valve	0.17
1185	Normal, 98% slide valve	0.23
1185	2 cold cylinders, unloaded	0.26
1185	1 cold cylinder, unloaded	0.21
1185	1 cold cylinder, max slide valve	0.29

3.3 Package vibration performance

3.3.1 Overall vibration

Example velocity running RMS example trends plotted against the relevant acceptability limits during operating conditions such as that shown in Figure 3b are presented in Figure 7. It can be observed that, in general, the vibration of the engine increases along with compressor loading while the opposite is true for the compressor, with the lowest vibration levels seen during full load. A summary of the overall package vibration under the steady-state, full load operating condition is presented in Table 6. The system was operating within limits at all locations.

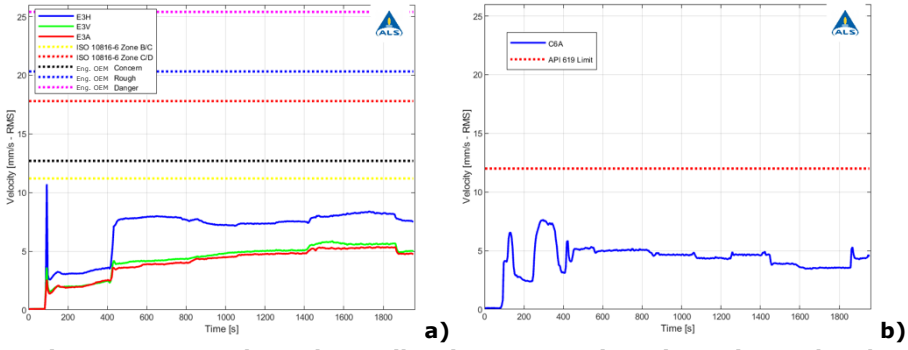

Figure 7 – Example package vibration RMS at a) Engine Drive End and b) Compressor Male Rotor

Table 6 – Overall package vibration velocities under full load

Location	mm/s (RMS)		
	Axial	Horizontal	Vertical
A1	2.5	5.7	3.6
A2	-	4.8	2.3
A3	5.3	8.4	5.6
A4	-	7.0	-
A5	-	9.5	-
A6	-	4.9	-
A7	-	5.6	-
A8	5.6	4.2	3.9
A9	3.6	3.1	2.9
A10	4.7	6.5	4.7
A11	-	2.3	-
A12	-	2.0	-
A13	-	3.5	-

3.3.2 Waterfall analysis

A summary of the natural frequencies identified from waterfall plots, examples of which are shown in Figure 8 again for the engine and compressor, is presented in Table 7. The natural frequencies were identified by looking for signs of amplitude amplification during the run-up phase. The excitation source and dominant direction for those natural frequencies were also identified. From the table summary, all of the natural frequencies coinciding with a dominant excitation source showed sufficient separation margin of greater than 10%.

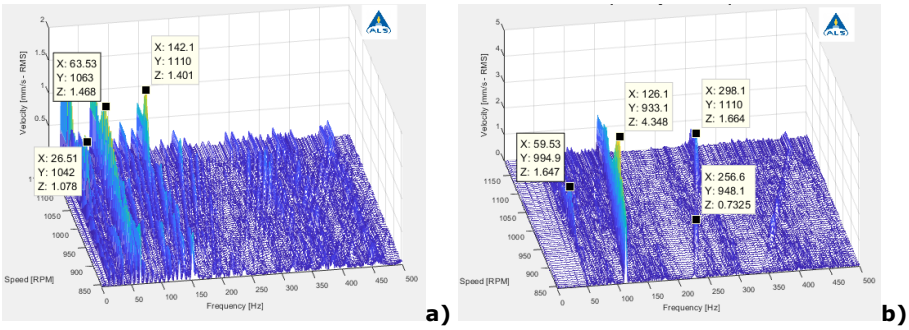

a) b)

Figure 8 – Example package vibration waterfalls for no-load run-up at a) Eng. Drive End – Shaft Centerline (axial) and b) Comp. Male Rotor – Axial

Table 7 – Overall package vibration velocities under full load

Sens.	Suspected natural frequencies (Hz)			Excit. source @ 1185 rpm		Sep. margin (%)	Comments
	X	Y	Z	(order)	(Hz)		
A3	26.5	26.5	26.5	1.5	29.6	10.5	Significant amplif. in horizontal
	63	-	-	3.5	69.1	8.9	Minor
	142	-	142	7.5	148.1	4.1	Minor
	-	-	195	10.5	207.4	6.0	Minor
A8	-	40	-	2.5	49.4	19.0	Minor
	59	-	-	3.5	69.1	14.6	Minor, possibly from engine frame
	-	-	80	4.5	88.9	10.0	Minor
	126	126	-	7.86	155.2	18.8	Significant amplif. in axial
	251	251	251	15.73	310.7	19.2	Minor
A13	59	-	-	3.5	69.1	14.6	Minor, possibly from engine frame
	126	-	-	7.86	155.2	18.8	Significant amplif. in axial
	256	-	-	15.73	310.7	17.6	Minor
	298	-	-	15.73	310.7	4.1	Minor

3.3.3 Effect of increasing load

In general and as expected, the engine vibration at dominant frequencies increases with increasing valve position. The engine vibration showed an increase in half order harmonics, particularly at orders 1.5, 2.5, 3.5, 4.5 and 6 (Figure 9a). The trend at those frequencies was also seen in the torsional vibration data, measured both by the strain gauges and the laser vibrometer, the latter as shown in Figure 6 and summarised in Table 5. It can be deduced that the engine vibration is directly correlated to the amount of loading imparted by the driven machinery. Meanwhile, the compressor dominant frequencies were found to decrease with increasing valve position, particularly at the lobe pass frequency (LPF) and harmonics as shown in in Figure 9b, again consistently with the torsional vibration. It can be hypothesized that loading of the screw compressor creates a damping effect on LPF related vibration.

3.3.4 Effect of cold cylinders

Investigation of the effect of inducing cold cylinders on the package vibration showed that the most sensitive location to detect an increase in torsional vibration in the engine through the monitoring of package vibration, was at the non-drive end of the

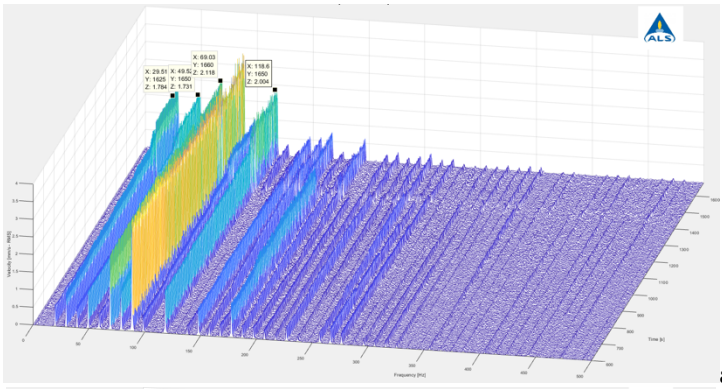

a)

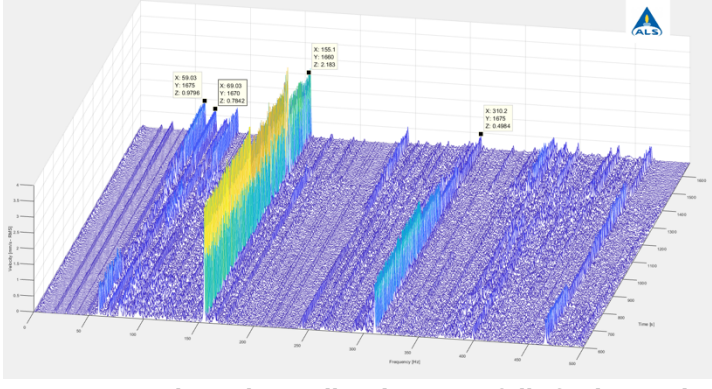

b)

Figure 9 – Example package vibration waterfalls for increasing load (20-98% slide valve), a) Eng. Non-Drive End and b) Comp. Male Rotor

engine (i.e. at the front of the engine) in the horizontal direction. A similar observation was made of the compressor vibration spectra at the drive end – horizontal (gearbox input). This is to be expected since this shaft is physically coupled to the engine crankshaft. All other locations across the compressor casing did not show any significant changes upon inducing of cold cylinders, indicating that they are less sensitive to the torsional vibrations of the crankshaft system.

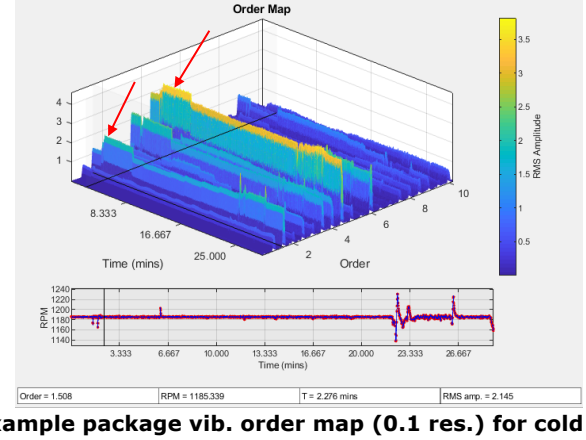

Figure 10 – Example package vib. order map (0.1 res.) for cold cyls. at Eng. Non-Dr. End; note incr. at orders 1.5 and 4.5 upon inducing two cold cyls.

Table 8 – Example package vib. vels. for cold cyls. at Eng. Non Dr. End

Order	mm/s (RMS)			
	Normal, unloaded	2 cold cylinders, unloaded	1 cold cylinder, unloaded	1 cold cylinder, full load
1.5	1.3	2.2	1.6	2.0
3.5	2.3	2.3	1.6	1.8
4.5	3.0	3.6	3.2	3.3

As shown in Figure 10, significant differences in the order 1.5 (c29.5 Hz), 3.5 (c69 Hz) and 4.5 (c88 Hz) frequencies occur upon inducing a cold cylinder. The results are summarized in Table 8 with the observation also in general agreement with the corresponding trend in torsional vibration data presented previously. It is postulated that the non-drive end of the engine is most sensitive to changes in torsional vibrations because of the presence of a torsional antinode or point of maximum vibratory twist at the damper housing as set out in section 2. Monitoring the trend of these vibrations could be an appropriate method of correlating package vibration to torsional vibration.

4. CONCLUSIONS

This paper has comprehensively reported an industrial vibration measurement campaign on an engine-compressor package, employing simultaneous measurement of torsional and package vibration. Significant insights into the preparation of the instrumentation, data acquisition and processing, in the context of the expected nature of the vibratory performance and documented limits of the system, have been detailed. The interaction of driven frequencies and structural resonances has been described in the context of an order 1.5 dominant peak and the first torsional natural frequency that were shown to lead to higher vibration at low vs. at high idle. The assessment and correlation of torsional and package vibration frequencies and levels, for increasing load and for induced cold cylinders, was presented. Finally, recommendations are made for the location (non-drive end of the engine and drive end of the equipment) and interpretation of *package* vibration measurements for the evaluation of *torsional* vibration. It is proposed that, in place of costly and time-consuming vibratory torque measurements, package vibration and/or rotational LDV measurements can reliably assess torsional vibration in an industrially valid context.

REFERENCES

(1) Downham, E., Woods, R., "The rationale of monitoring vibration on rotating machinery in continuously operating process plant", *Trans. ASME J. of Engineering for Industry* 71-Vibr-96, 1971.
(2) Mitchell, J. S., "Vibration analysis - its evolution and use in machinery health monitoring", *Soc. Env. Eng. Symp. Machine Health Monitoring*, London, 1975.
(3) Tawadros, P, Awadallah, M, Walker, PD, Zhang, N, "Using a low-cost bluetooth torque sensor for vehicle jerk and transient torque measurement", *Proc. IMechE, Part D: J. Auto Eng.*, 2019.
(4) Rothberg, S.J., et al., "An international review of laser Doppler vibrometry: making light work of vibration measurement", *Opt. Lasers in Eng.* 99, 2017.
(5) Halkon, B.J., Rothberg, S.J., "A practical guide to laser Doppler vibrometry measurements directly from rotating surfaces", *Proc. Eleventh Int. Conf. on Vibs. Rot. Mach., Manc., UK,* 2016, pp. 215-230, pp. 9-16.
(6) HBM, "Pre-wired strain gauges, model 350 CLY4-3L-3M" www.hbm.com/en/4550/pre-wired-strain-gauges-fast-safe-and-convenient [accessed 13-03-20].
(7) Binsfield Eng., Inc. "TorqueTrak 10K Torque Telemetry System" binsfeld.com/wp-content/uploads/2019/08/TT-10K_8695003_E.pdf [accessed 21-02-20].
(8) Polytec GmbH, "Rotational Laser Vibrometer RLV-5500 Operating Instructions" (41278-Man-RotVib-RLV5500-1116-05en), 2016.
(9) Kistler Instrument. Corp., "Ceramic Shear Triaxial Accelerometer type 8763B" www.kistler.com/?type=669&fid=10&model=download [accessed 13-03-20].
(10) CTC, Inc., "AC102 - Multi-Purpose Accelerometer" www.ctconline.com/ctc_100_mv_g_standard_size_accelerometers.aspx?prd=AC102 [accessed 13-03-20].
(11) Døssing, O., "Structural Testing, Part 1 – Mechanical Mobility Measurements", Brüel & Kjær, Denmark, 1988.
(12) Nat. Instruments, "NI cDAQ™-9178 Specifications, NI CompactDAQ Eight-Slot USB Chassis" www.ni.com/pdf/manuals/374046a.pdf [accessed 24-02-20].
(13) ISO 10816-6:1995(en), "Mechanical vibration — Evaluation of machine vibration by measurements on non-rotating parts — Part 6: Reciprocating machines with power ratings above 100 kW", 1995.
(14) API STD 619, "Rotary-Type Positive-Displacement Compressors for Petroleum, Petrochemical, and Natural Gas Industries", Fifth Edition, 2010.
(15) ABSignal, Inc., "ModalVIEW – modal testing & analysis tool" absignal.com/product/index.php [last accessed 01-03-20].